BIOMETRICS DOI: 10.1111/biom.12766

Spatial Capture–Mark–Resight Estimation of Animal Population Density

Murray G. Efford[1,*] and **Christine M. Hunter**[2,**]

[1]Department of Mathematics and Statistics, University of Otago, P.O. Box 56, Dunedin, New Zealand
[2]Department of Conservation, Private Bag 5, Nelson 7042, New Zealand
*email: murray.efford@otago.ac.nz
**email: chunter@doc.govt.nz

SUMMARY. Sightings of previously marked animals can extend a capture–recapture dataset without the added cost of capturing new animals for marking. Combined marking and resighting methods are therefore an attractive option in animal population studies, and there exist various likelihood-based non-spatial models, and some spatial versions fitted by Markov chain Monte Carlo sampling. As implemented to date, the focus has been on modeling sightings only, which requires that the spatial distribution of pre-marked animals is known. We develop a suite of likelihood-based spatial mark–resight models that either include the marking phase ("capture–mark–resight" models) or require a known distribution of marked animals (narrow-sense "mark–resight"). The new models sacrifice some information in the covariance structure of the counts of unmarked animals; estimation is by maximizing a pseudolikelihood with a simulation-based adjustment for overdispersion in the sightings of unmarked animals. Simulations suggest that the resulting estimates of population density have low bias and adequate confidence interval coverage under typical sampling conditions. Further work is needed to specify the conditions under which ignoring covariance results in unacceptable loss of precision, or to modify the pseudolikelihood to include that information. The methods are applied to a study of ship rats *Rattus rattus* using live traps and video cameras in a New Zealand forest, and to previously published data.

KEY WORDS: Capture–mark–resight model; Density estimation; Maximum likelihood; Overdispersion; Spatial mark–resight; Spatially explicit capture–recapture.

1. Introduction

Capture–recapture is an extensive set of methods for estimating the abundance and other parameters of animal populations from incomplete samples. All rely on distinguishing individuals by marks that may be either naturally occurring (such as DNA or pelage differences) or applied during the study. When an individual is detected for the first time it joins the pool of known, marked individuals and any further records contribute to its "capture history." However, it is often desirable for reasons of cost, practicality or animal welfare to collect sighting data without marking new animals; previously marked animals are individuated, allowing the development of individual capture histories, but unmarked animals are only counted. Such data cannot be analyzed with conventional capture–recapture models. Methods for non-spatial "mark–resight" data have been extended and refined in the last decade by McClintock and coworkers (McClintock et al., 2009a,b; McClintock and White, 2009, 2012; McClintock et al., 2014) and are now in widespread use. Analyses of spatially-referenced mark–resight data have been proposed recently (Sollmann et al., 2013b; Royle et al., 2014); these have the advantage of providing rigorous estimates of population density and the number of animals in a specified region. Application of spatial mark–resight (SMR) models so far has been limited, perhaps because of the need for custom model construction and the computational overheads of Markov chain Monte Carlo sampling (MCMC).

The two dominant strategies for fitting spatially explicit capture–recapture (SECR) models carry over into SMR. Borchers and Efford (2008) described a likelihood-based method for SECR requiring integration over the unknown locations of individual activity (home-range) centres; centres were assumed to arise from a known spatial point process, specifically a (possibly inhomogeneous) 2-D Poisson process. Royle and coworkers (Royle and Young, 2008; Royle et al., 2014) fitted essentially the same models in a Bayesian context by treating the unknown locations of marked individuals as numerous latent variables, augmented by an arbitrary number of locations for unmarked and potentially existant individuals. The Bayesian approach has been applied to SMR data by Sollmann et al. (2013a,b), Rich et al. (2014) and others.

The development of SMR methods faces two major challenges. Firstly, previous mark–resight methods, both spatial and non-spatial, have generally assumed that the sighting probabilities of pre-marked individuals do not differ systematically from the population as a whole. This holds when the marked animals are a random sample. However, the marking process itself often relies on spatial sampling, possibly using a stationary grid of traps, and the assumption is then almost certainly false because animals close to the traps are likely to predominate in the marked sample. The marking process thus induces differing spatial structure in the marked and unmarked populations (Figure 1) that should be accounted for when modeling sightings. The direct solution is to collect data from both the marking and sighting phases, and to jointly model both processes. This approach was applied to nonspatial data by Matechou et al. (2013) and is developed here for spatial data. A compromise solution is to specify an assumed spatial distribution for the marked animals, and implicitly also for the unmarked animals, while modeling only the sighting data spatially (e.g., Sollmann et al., 2013b). The problem with this compromise is that the actual distribution of marked animals is unknown and its mis-specification may lead to substantial bias in the estimates. We use "spatial capture–mark–resight" (SCMR) for models that include the marking phase, and "spatial mark–resight" (SMR) for models that do not.

The second challenge is specific to estimation by maximum likelihood. Sightings of unmarked animals are by definition not attributed to individuals, so modeling this component of the data requires a different approach to modeling the spatial detection histories of individuals. This is because each detection history is associated with a unique (if unknown) activity center, but we cannot parse the aggregate unmarked counts to know how many centres to model. In the latent-variable approach of Sollmann et al. (2013b) and Chandler and Royle (2013) it is straightforward to model (essentially to simulate) the latent sightings of the (augmented) population of unmarked individuals.

This automatically induces the spatial structure in the counts that results from the clustering of detections around the randomly located center of each individual. In the MLE framework, each observed aggregated count may be modeled as a Poisson variate whose expected value depends on the location of the detector. However, the detector-specific Poisson processes are correlated (together they follow a multivariate Poisson process) and ignoring the multivariate nature of the counts has consequences for the parameter estimates. Chandler and Royle (2013) showed that there can be enough information in the spatial correlation structure of counts to obtain crude estimates of density and spatial detection parameters by data augmentation and MCMC. Discarding this information from the likelihood potentially leads both to bias and loss of real precision, and to a spurious increase in apparent precision due to overdispersion. We suggest using a pseudolikelihood that is a weighted combination of the likelihood components for marked and unmarked animals. The performance of the maximum pseudolikelihood estimator (MPLE) is superior to the naive MLE and approaches that of the full model fitted by data augmentation and MCMC.

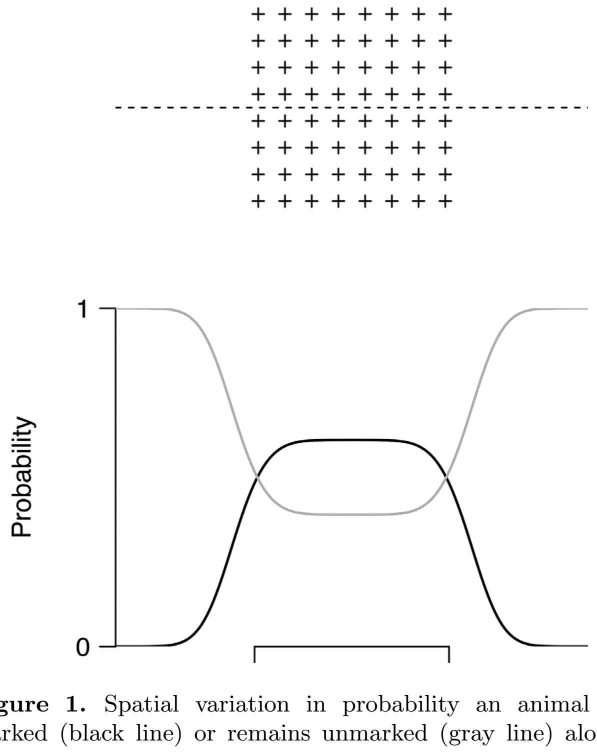

Figure 1. Spatial variation in probability an animal is marked (black line) or remains unmarked (gray line) along a notional transect (dashed) across a capture–recapture grid. Computed for a single marking occasion with $h_0 = 0.15$ and σ = detector spacing (half-normal detection function). The spatial distribution of marked animals is central to spatial mark–resight models.

Our goal in this article is to develop a suite of SCMR and SMR models that may be fitted by maximizing the likelihood, following the approach to SECR of Borchers and Efford (2008) and Efford, Borchers, and Byrom (2009). Section 2 introduces notation and outlines the foundation provided by likelihood-based SECR. Section 3 presents the likelihood for the SCMR model and Section 4 does the same for the SMR model. Various extensions and special cases are considered along with implementation issues in Section 5. Section 6 applies the method to a novel rat dataset. Simulations to assess the performance of the proposed methods are presented in Section 7 and the Supplementary Materials, which also reanalyze published data on grassland sparrows *Ammodramus savannarum* and *A. henslowii* in Pennsylvania and puma *Puma concolor* in Central and South America. Some issues arising are discussed in Section 8.

2. SECR Framework and Notation

Much of the structure of our models is shared with the SECR models of Borchers and Efford (2008), Efford, Borchers, Byrom (2009), and Borchers and Fewster (2016), and we start by outlining their common features.

2.1. *Detector Locations*

Data are assumed to be collected at pre-determined points or by searching disjoint polygonal areas. Detectors are of two general types (marking and sighting); it is assumed that detectors are positioned so that some individuals are exposed to both types, except in SMR (sighting-only) analyses that we consider later.

2.2. *Detection Histories*

The data comprise the n detection histories of marked animals, including any resightings, and counts of the sightings of unmarked animals at each detector in each sampling interval (occasion) j $(1 \leq j \leq J)$. A detection history $\boldsymbol{\omega}_i$ codes the status of marked individual i on each occasion with respect to each detector k $(1 \leq k \leq K)$. We use $\boldsymbol{\omega}_i$ in the inclusive sense of Efford, Dawson, and Borchers (2009): an observation on a particular individual i may be binary $(\omega_{ijk} \in \{0, 1\})$ or a count of detections $(\omega_{ijk} \in \{0, 1, 2, \ldots\})$ depending on the detector type, and may include auxiliary data, such as the coordinates of each detection within searched polygons (Royle and Young, 2008; Efford, 2011). For model development, we focus on count data from point detectors; $\boldsymbol{\omega}$ is the set of observed detection histories.

2.3. *Density Model*

The animal population is represented by a 2-dimensional inhomogenous Poisson spatial point process. Each point corresponds to the home-range center of an individual animal. Centres are assumed fixed for the duration of sampling (marking and resighting), and the population is closed (no animals join or leave). The point process is represented by $\lambda(\mathbf{s};\boldsymbol{\beta})$ where $\mathbf{s}$ is the vector of coordinates (x, y) for a point in the plane and $\boldsymbol{\beta}$ is a vector of parameters used to model spatial trend in intensity or dependence on spatial covariates. The homogeneous Poisson is a special case in which λ is a constant—the uniform intensity of the process—and $\boldsymbol{\beta}$ is a scalar.

2.4. *Detection Functions*

We assume that the cumulative hazard of detection at detector k on occasion j declines with the distance $d_{ik} = ||\mathbf{s}_i - \mathbf{l}_k||$ between the detector location $\mathbf{l}_k$ and an animal's home-range center $\mathbf{s}_i$. Formally, $H_{ijk} = h(d_{ik};\boldsymbol{\theta})$, where $\boldsymbol{\theta}$ is a vector of parameters for the detection function h. We also express this as $H_{jk}(\mathbf{s}_i)$. The most commonly used function is the half-normal $H_{ijk} = h_0 \exp\{-d_{ik}^2/(2\sigma^2)\}$ with parameters h_0 and σ that may vary with detector or occasion, particularly between marking and resighting occasions. Individuals are assumed not to differ with respect to $\boldsymbol{\theta}$ although extensions to include a random effect are feasible as discussed in Section 8.

3. Spatial Capture-Mark-Resight Likelihood

M represents the subset of occasions on which any new individuals are marked, and R represents sighting occasions. We focus initially on detectors that yield count data and extend later to binary detection histories. We consider a joint likelihood of the form

$$L(\boldsymbol{\beta}, \boldsymbol{\theta}|\boldsymbol{\omega}, \mathbf{T}) = L_M(\boldsymbol{\beta}, \boldsymbol{\theta}|\boldsymbol{\omega}) \times L_T(\boldsymbol{\beta}, \boldsymbol{\theta}|\mathbf{T}), \tag{1}$$

where $\mathbf{T}$ is the $J \times K$ matrix of unmarked sightings. This formulation presumes that the marked and unmarked animals on any sampling occasion comprise distinct spatial populations whose detections can be modeled independently. We later also consider the possibility that some sightings were of marked animals that were not individually identified and therefore could be recorded only as aggregated counts ($\mathbf{T}'$). For clarity, we omit the dependence of expressions on parameters after the first reference.

3.1. *Marking and Sightings of Marked Animals*

The likelihood associated with marked animals has the form

$$L_M(\boldsymbol{\beta}, \boldsymbol{\theta}|\boldsymbol{\omega}) = \Pr(n; \boldsymbol{\beta}, \boldsymbol{\theta}) \times \Pr(\boldsymbol{\omega}|n; \boldsymbol{\beta}, \boldsymbol{\theta}). \tag{2}$$

Animals appear in the marked sample with location-dependent probability $p(\mathbf{s}_i; \boldsymbol{\theta}) = 1 - \exp\{-H(\mathbf{s}_i; \boldsymbol{\theta})\}$, where $H(\mathbf{s}_i) = \sum_{j \in M} \sum_k H_{jk}(\mathbf{s}_i)$. This follows Borchers and Efford (2008) and Borchers and Fewster (2016) except for the restriction to a subset of occasions on which new individuals are marked. The number of animals detected n is univariate Poisson with parameter $\Lambda(\boldsymbol{\beta}, \boldsymbol{\theta}) = \int_{\mathbb{R}^2} \lambda(\mathbf{s}) p(\mathbf{s})\, d\mathbf{s}$. Alternatively, a fixed number of centres N may be distributed within a defined region A; n is then a binomial sample from N with inclusion probability $\int_A \lambda(\mathbf{s}) p(\mathbf{s})\, d\mathbf{s} \,/\, \int_A \lambda(\mathbf{s})\, d\mathbf{s}$.

For the second probability in (2), we assume independence among animals, and hence

$$\Pr(\boldsymbol{\omega}|n, \boldsymbol{\beta}, \boldsymbol{\theta}) = \binom{n}{n_1, \ldots, n_C} \prod_{i=1}^{n} \Pr(\boldsymbol{\omega}_i; \boldsymbol{\beta}, \boldsymbol{\theta})$$

where $n_1, \ldots, n_C$ are the frequencies of the C unique detection histories. Adapting Borchers and Efford (2008), we have

$$\Pr(\boldsymbol{\omega}_i) = \int_{\mathbb{R}^2} \Pr(\boldsymbol{\omega}_i|\mathbf{s})\ f(\mathbf{s}; \boldsymbol{\beta}, \boldsymbol{\theta})\ d\mathbf{s}, \tag{3}$$

where $\Pr(\boldsymbol{\omega}_i|\mathbf{s}) = p(\mathbf{s})^{-1} \prod_j \prod_k \Pr(\omega_{ijk}|\mathbf{s})$, and the probability density function for the location of a marked animal is $f(\mathbf{s}) = \frac{\lambda(\mathbf{s})p(\mathbf{s})}{\Lambda}$. Note that p, Λ, and f depend only on $\boldsymbol{\beta}$ and $\boldsymbol{\theta}$ for occasions $j \in M$.

The form of $\Pr(\omega_{ijk})$ depends on whether j is a marking or resighting occasion. We introduce a parameter p_I for the probability that a sighting of a marked animal will be attributable to an individual. Detections of each animal at each detector arise from a Poisson process with parameter $H_{jk}(\mathbf{s})$ for $j \in M$, and parameter $p_I \delta_{ij}^{-} H_{jk}(\mathbf{s}_i)$ for $j \in R$, where δ_{ij}^{-} is 1 if animal i was marked before j and 0 otherwise. Unidentified sightings of marked animals are counted, but not individuated; they are modeled separately in Section 3.3.

3.2. *Sightings of Unmarked Animals*

The observations on unmarked animals are counts of the number of detections in each interval j at each detector k, aggregated across individuals (T_{jk}). If the distribution of activity centres is an inhomogenous 2-dimensional Poisson process, then we expect the number of detections at a point to follow a univariate Poisson distribution (Borchers and Efford, 2008). The expected number μ_{jk} depends on the local intensity of the population process $\lambda(\mathbf{s}; \boldsymbol{\beta})$ and the site-specific detection rate, discounting animals marked before j ($p^{-}(\mathbf{s}_i, j; \boldsymbol{\theta}) = 1 - \exp\{-\sum_{l \in M, l<j} \sum_k H_{jk}(\mathbf{s}_i; \boldsymbol{\theta})\}$) :

$$\mu_{jk} = \int_{\mathbb{R}^2} \lambda(\mathbf{s})\, \{1 - p^{-}(\mathbf{s}, j)\}\, H_{jk}(\mathbf{s})\, d\mathbf{s}. \tag{4}$$

This theory describes detections at one detector. For an array of detectors, it is tempting to assume independence between sightings on successive occasions and at different detectors. The likelihood is then easily formulated as $L_T(\boldsymbol{\beta}, \boldsymbol{\theta}|\mathbf{T}) = \prod_{j \in R} \prod_k \Pr(T_{jk}|\mu_{jk})$ where $\mathbf{T}$ is the entire matrix of sighting data. However, for a particular realization of the population process, the T_{jk} are spatially correlated: neighboring detectors within the home range of one or more animals share a high probability of detecting animals, and the configuration of home ranges is assumed constant over occasions. One consequence is that the variance of the sum $T = \sum_j \sum_k T_{jk}$ across different realizations of the population process exceeds its mean, that is, T is overdispersed relative to a Poisson distribution. Another is that the correlations carry information about the spatial scale of detection σ, which can be exploited to provide density estimates even in the absence of individual marks or external data on the scale of detection (Chandler and Royle, 2013). Models to "capture" the spatial correlation in counts of unmarked animals at present require detailed accounting for the latent locations of individuals, as in the Bayesian data augmentation approach of Chandler and Royle (2013).

We bypass this obstacle to ML estimation by discarding the spatial information in the covariance structure. Estimates of $\boldsymbol{\beta}$ and $\boldsymbol{\theta}$ may be obtained by maximizing (1) using only a "naive" Poisson model for the unmarked animals (i.e., $L_T = \mu^T \exp(-\mu)/T!$, where $\mu = \sum_j \sum_k \mu_{jk}$). Mis-specification causes T to be overdispersed relative to the Poisson model; we call this "spatial overdispersion" to distinguish it from overdispersion from other causes (heterogeneity among individuals, sightings not independent in time, etc.). For many scenarios the naive MLE are nearly unbiased despite the mis-specification, as we show by simulation in Section 7 and Web Appendix A. However, it is inescapable that spatial overdispersion in T will bias estimates of the sampling variance based on the Hessian evaluated at the naive MLE, and that coverage of confidence intervals will suffer. To address this problem, we define a pseudolikelihood that includes an adjustment for spatial overdispersion c:

$$L_c(\boldsymbol{\beta}, \boldsymbol{\theta}|\boldsymbol{\omega}, \mathbf{T}) = L_M(\boldsymbol{\beta}, \boldsymbol{\theta}|\boldsymbol{\omega}) \times L_T(\boldsymbol{\beta}, \boldsymbol{\theta}|\mathbf{T})^{1/c}. \qquad (5)$$

Spatial overdispersion may be estimated by simulating $\{T_{jk}\}$ for a large number of realizations of the population process, using estimates of $\boldsymbol{\beta}$ and $\boldsymbol{\theta}$ from an initial model fit, and computing $\hat{c} = \text{var}(T)/\text{mean}(T)$.

In summary, we propose a 3-step process: (i) obtain the MLE using a naive likelihood that ignores covariance of the unmarked counts, (ii) estimate spatial overdispersion (c) at the naive MLE, and (iii) re-fit the model using $\hat{c}$ in the pseudolikelihood (5).

3.3. *Sightings of Marked Animals not Individually Identified*

The likelihood can be extended to include sightings $\mathbf{T}'$ of animals that were seen to be marked, but whose identity was not determined. We initially considered an independent likelihood component $L_{T'}(\boldsymbol{\beta}, \boldsymbol{\theta}|\mathbf{T}')$, where T_{jk} is Poisson with expected value $\mu'_{jk} = (1-p_I)\int_{\mathbb{R}^2} \lambda(\mathbf{s}) H_{jk}(\mathbf{s}) p^{-}(\mathbf{s}, j)\, d\mathbf{s}$. However, it is more efficient to condition on the n marked animals, each available for sighting from the time it was marked. The new likelihood component for marked animals is then

$$L'_M(\boldsymbol{\beta}, \boldsymbol{\theta}|\boldsymbol{\omega}, \mathbf{T}') = \Pr(n; \boldsymbol{\beta}, \boldsymbol{\theta}) \times \Pr(\boldsymbol{\omega}|n; \boldsymbol{\beta}, \boldsymbol{\theta}) \times \Pr(\mathbf{T}'|\boldsymbol{\omega}; \boldsymbol{\beta}, \boldsymbol{\theta}). \qquad (6)$$

The expected number of unidentified marked individuals is

$$\mu'_{jk} = (1-p_I)\sum_{i=1}^{n} \delta^{-}_{ij} \int_{\mathbb{R}^2} f(\mathbf{s}_i|\boldsymbol{\omega}_i)\, H_{jk}(\mathbf{s})\, d\mathbf{s}, \qquad (7)$$

where $f(\mathbf{s}_i|\boldsymbol{\omega}_i)$ is the probability density for the location of animal i, given its detection history, and δ^{-}_{ij} is an indicator for capture before j. Using $t(\boldsymbol{\omega}_i, \mathbf{s}) = \Pr(\boldsymbol{\omega}_i|\mathbf{s})\lambda(\mathbf{s})$ and $f(\mathbf{s}_i|\boldsymbol{\omega}_i) = t(\boldsymbol{\omega}_i, \mathbf{s})/\int_{\mathbb{R}^2} t(\boldsymbol{\omega}_i, \mathbf{s})\, d\mathbf{s}$ (cf. Borchers and Efford, 2008, p. 380), we have

$$\mu'_{jk} = (1-p_I)\sum_{i=1}^{n} \delta^{-}_{ij} \int_{\mathbb{R}^2} t(\boldsymbol{\omega}_i, \mathbf{s})\, H_{jk}(\mathbf{s})\, d\mathbf{s} \Big/ \int_{\mathbb{R}^2} t(\boldsymbol{\omega}_i, \mathbf{s})\, d\mathbf{s}. \qquad (8)$$

If $p_I = 1$ then all marked animals are identified and this component drops out of the likelihood. Spatial overdispersion may be allowed for in the pseudolikelihood (5) by raising $\Pr(\mathbf{T}'|\boldsymbol{\omega})$ to a suitable power estimated by simulation as for L_T.

4. Spatial Mark–Resight Likelihood (Sighting-Only)

To this point, we have assumed that information is available on the distribution of effort and location of detections on the marking occasions. Conventional non-spatial mark–resight methods avoid this requirement by conditioning on the number of pre-marked animals n_0, without modeling how they came to be marked, and make the further assumption that the marked animals are a random sample from the entire (non-spatial) population (McClintock and White, 2012; McClintock et al., 2014). The assumption is carried over explicitly in the spatial model of Sollmann et al. (2013b) for data that do not include the marking phase, and discussed further by Royle et al. (2014). Sighting-only models may be appropriate when the marking process is unknown, but likely to be spatially uniform. This could apply when a fraction of individuals are born with distinguishing marks or acquire them naturally (e.g., Rich et al., 2014).

In this section, we develop a version of the spatially explicit mark–resight likelihood that conditions on previous marking. The data comprise observed sighting histories $\boldsymbol{\omega}$ of n marked individuals, as well as the sighting matrices $\mathbf{T}$ and possibly $\mathbf{T}'$ ($p_I < 1$). Marking is assumed to have been completed prior to sampling, so all occasions are sighting occasions. We consider two scenarios: the number of marked individuals present in the population at the time of sampling may be known, in which case $n = n_0$ and the data may include all-zero detection histories, or n_0 may be unknown and the data include detection histories only for re-sighted animals ($n \leq n_0$). The key requirement for both scenarios is that the spatial distribution of the n_0 marked individuals is known at the time of sampling.

4.1. *Mark–Resight with Known Number of Marked Individuals*

Assume the n_0 marked individuals have a known spatial distribution with probability density $\pi(\mathbf{s})$. Using only sightings of marked animals, we can estimate the vector of detection parameters $\boldsymbol{\theta}$ by maximizing the likelihood conditional on n_0

and π:

$$\begin{aligned} L_S(\boldsymbol{\theta}|n_0, \boldsymbol{\omega}, \pi) &= \Pr(\boldsymbol{\omega}|n_0, \pi; \boldsymbol{\theta}) \\ &= \binom{n_0}{n_1, \ldots, n_C} \prod_{i=1}^{n_0} \int_{\mathbb{R}^2} \pi(\mathbf{s}) \Pr(\boldsymbol{\omega}_i|\mathbf{s}) \, d\mathbf{s}. \quad (9) \end{aligned}$$

with $\boldsymbol{\omega}_i$ and $n_1, \ldots, n_C$ defined as before. However, in order to estimate the population parameter $\boldsymbol{\beta}$, we must include sightings of unmarked animals $\mathbf{T}$ in the joint likelihood:

$$L(\boldsymbol{\beta}, \boldsymbol{\theta}|n_0, \boldsymbol{\omega}, \mathbf{T}, \pi) = \Pr(\boldsymbol{\omega}|n_0, \pi; \boldsymbol{\theta}) \times \Pr(\mathbf{T}|n_0, \pi; \boldsymbol{\beta}, \boldsymbol{\theta}). \quad (10)$$

The expected number of sightings of unmarked animals at detector k on occasion j is

$$\mu_{jk} = \int_{\mathbb{R}^2} \{\lambda(\mathbf{s}) - n_0 \pi(\mathbf{s})\} H_{jk}(\mathbf{s}) \, d\mathbf{s}, \quad \lambda(\mathbf{s}) \geq n_0 \pi(\mathbf{s}), \quad (11)$$

where $H_{jk}(\mathbf{s})$ is the occasion- and detector-specific expected number of sightings of an individual at $\mathbf{s}$, as before.

Sightings of marked animals that were not individually identified ($\mathbf{T}'$) relate to n individuals for which we have some observed locations (allowing us to apply (8)) and $n_0 - n$ other individuals that were marked and never sighted. Thus, overall

$$\mu'_{jk} = (1 - p_I) \sum_{i=1}^{n_0} \int_{\mathbb{R}^2} \Pr(\omega_i|\mathbf{s}) \pi(\mathbf{s}) H_{jk}(\mathbf{s}) \, d\mathbf{s} \Big/ \int_{\mathbb{R}^2} \Pr(\omega_i|\mathbf{s}) \pi(\mathbf{s}) \, d\mathbf{s}. \quad (12)$$

For all $n_0 - n$ unsighted individuals $\Pr(\omega_i|\mathbf{s}) = \exp\{-H(\mathbf{s})\}$, allowing these to be aggregated in the term $(n_0 - n) \int_{\mathbb{R}^2} \exp\{-H(\mathbf{s})\} \pi(\mathbf{s}) H_{jk}(\mathbf{s}) \, d\mathbf{s} / \int_{\mathbb{R}^2} \exp\{-H(\mathbf{s})\} \pi(\mathbf{s}) \, d\mathbf{s}$, with summation only over the n sighted individuals. In the special case that the centres of marked animals are distributed uniformly over a known region A_0 with area $[A_0]$, $\pi(\mathbf{s})$ takes the value $1/[A_0]$ inside that region and 0 outside. The integrals in equations (9) and (12) then need only be evaluated over A_0, and (11) is seen to have two components, one for all animals outside A_0 and one for the animals inside A_0 that escaped marking.

4.2. *Mark–Resight with Unknown Number of Marked Individuals*

The number of marked individuals that remain in the study population at the time of sighting surveys will be unknown if enough time has passed to allow significant mortality or emigration. The total number of marks may also be unknown if the study relies on natural marks and some animals are not identifiable because they lack distinctive marks (Rich et al., 2014). When the number of marked individuals is unknown, n refers to the number of observed (not all-zero) sighting histories, and the likelihood component associated with sightings of marked animals follows (2) more closely than (9), owing to the need to allow for the unobserved (all-zero) histories of some marked animals. This is directly analogous to the use of a zero-truncated Poisson distribution by McClintock et al. (2009a) in the corresponding non-spatial case.

We assume that the marked animals present at the time of sampling remain distributed as $\pi(\mathbf{s})$. Previously marked animals appear in the sighting sample with site-dependent probability $p(\mathbf{s})$ as before. We define an effective sampling area for the population of marked animals as $a_0(\boldsymbol{\theta}) = \int_{\mathbb{R}^2} \pi(\mathbf{s}) p(\mathbf{s}) d\mathbf{s}$. Then

$$L_S(\boldsymbol{\theta}|n, \boldsymbol{\omega}) = \binom{n}{n_1, \ldots, n_C} a_0(\boldsymbol{\theta})^{-n} \prod_{i=1}^{n} \int_{\mathbb{R}^2} \pi(\mathbf{s}) \Pr(\boldsymbol{\omega}_i|\mathbf{s}) \, d\mathbf{s}. \quad (13)$$

For the expected numbers of sightings, we substitute n/a_0 for n_0 in (11) and (12). No adjustment is required for animals not yet marked at time j because marking is completed before $j = 1$.

5. Extensions, Special Cases and Implementation

5.1. *Binary Data*

We have focussed on count data for both the marking and sighting phases. Data types may vary among occasions. In particular, the detector type may differ between marking occasions ($j \in M$) and sighting occasions ($j \in R$). Binary data ($\omega_{ijk} \in \{0, 1\}$) arise when animals are trapped and must be released before they can be caught again, or when repeated visits by an individual to a detector cannot be distinguished. It is difficult, for example, to distinguish multiple visits to a passive sampling device such as a DNA hair snare from a single visit on which multiple samples were left. So long as detections of different animals remain independent, each binary data type may be modeled by replacing the Poisson model for ω_{ijk} with a Bernoulli model whose sole parameter is q. For binary proximity detectors $q_{ijk} = 1 - \exp\{-H_{jk}(\mathbf{s}_i)\}$. For binary data from multi-catch traps the corresponding parameter is $q_{ijk} = [1 - \exp\{-H_j(\mathbf{s}_i)\}] \, H_{jk}(\mathbf{s}_i)/H_j(\mathbf{s}_i)$, where $H_j(\mathbf{s}_i) = \sum_k H_{jk}(\mathbf{s}_i)$.

A distinction is drawn between binary data on individuals (ω_{ijk}) and data that are binary at the level of a detector. For marked animals there is no reason to aggregate at the detector level, but for unmarked animals this is inevitable. Binary data on unmarked individuals record only whether at least one such individual visited a detector on a particular occasion ($T_{jk} \in \{0, 1\}$). The probability of this event is $r = 1 - \exp(-\mu_{jk})$, and the corresponding likelihood component is $L_T = \prod_{j \in R} \prod_k r^{T_{jk}} (1 - r)^{1 - T_{jk}}$.

5.2. *Marked Animals not Distinguished on Sighting Occasions*

If the sighting method does not allow marked animals to be distinguished from unmarked animals then the observations are summed "unresolved" counts, and sighting occasions do not contribute to the detection histories of marked animals. Unresolved counts are simply modeled by dropping the prior marking factor from equation (4), leading to $\mu_{jk} = \int_{\mathbb{R}^2} \lambda(\mathbf{s}) H_{jk}(\mathbf{s}) d\mathbf{s}$. The MPLE model is identifiable if at least one of the parameters h_0 and σ (most likely σ) is constant between marking and sighting occasions. The lack of information on detection parameters from sighting occasions is a serious impediment to the use of unresolved counts, but they may contribute to the estimation of spatial trend in density.

5.3. *Uniform-Density Population*

For a homogeneous 2-D Poisson distribution of centres $\lambda(\mathbf{s})$, (3) may be simplified because $p(\mathbf{s})$ terms cancel (Borchers and Efford, 2008, p. 379). Then

$$\Pr(\boldsymbol{\omega}|\mathbf{s}) = \binom{n}{n_1, \ldots, n_C} \prod_{i=1}^{n} \frac{\int_{\mathbb{R}^2} \Pr(\boldsymbol{\omega}_i|\mathbf{s}) d\mathbf{s}}{a(\boldsymbol{\theta})}$$

where $a(\boldsymbol{\theta}) = \int_{\mathbb{R}^2} p(\mathbf{s}) d\mathbf{s}$ and $\Pr(\boldsymbol{\omega}_i|\mathbf{s}) = \prod_j \prod_k \Pr(\boldsymbol{\omega}_{ijk}|\mathbf{s})$ as in Section 3.1.

If density can be assumed uniform then an alternative estimation strategy is to condition on the number of detected individuals. The likelihood from only the rightmost factor in equation (2) (the probability of observing $\boldsymbol{\omega}$ conditional on n) is maximized to estimate the detection parameter vector $\boldsymbol{\theta}$. A Horvitz–Thompson-like estimate of density is $\hat{\lambda} = n/a(\hat{\boldsymbol{\theta}})$ (Borchers and Efford, 2008). However, the inclusion of unmarked sightings $\mathbf{T}$ is problematic as their expected number (μ_{jk}) depends on density, which is not a parameter in the model (cf (4)).

5.4. *Implementation*

Estimates are obtained by maximizing the pseudolikelihood numerically. It is convenient to approximate the integrals as sums over small spatial pixels, and to restrict the summation to habitat in the vicinity of the detectors (i.e., to exclude non-habitat and places so distant that there is near-zero chance an animal centred there would have been detected). Maximization is over the logarithms of the parameters (or the logit in the case of p_I), and sampling variances and covariances of the transformed parameters are obtained from the Hessian matrix evaluated at the MPLE, or by a parametric bootstrap. Confidence limits are back-transformed from symmetrical (Wald) limits on the transformed scale; reported standard errors are delta-method approximations. An implementation is included in the R package "secr" (R Core Team, 2016; Efford, 2017). This also allows the user to model each parameter in more detail, for example, to express $\log(\lambda)$ as a linear function of pixel-specific habitat variables, or $\log(h_0)$ as varying among occasions.

6. *Example:* Population Density of Ship Rats in Southern Beech Forest

We analyzed unpublished data from a study of ship rats *Rattus rattus* living in a New Zealand forest. Rats were live-trapped and marked with individual tail tattoos over four days on a 10 × 10 grid of traps spaced 25 m apart, and then monitored over seven days with a matching grid of motion-activated video cameras, offset by about 5 m. On average only 73% of traps and 89% of cameras were operated each day. Of the 80 rats trapped and tattooed, only 13 were recaptured. However, 47 tattooed rats were identified a total of 497 times in the video recordings. Further sightings were assigned to the categories "Unmarked" (1374), "Marked, identity unknown" (878), and "Uncertain" (721). We discarded "Uncertain" sightings. Details and extended results are in Web Appendix C.

SCMR estimators (naive MLE and MPLE) were computed for the trapping and sighting data, both using full counts of unmarked sightings and with the sightings reduced to binary data (per detector per night). Estimates of c were obtained by simulating 10,000 sighting datasets from the naive fit. We also computed the MLE of density from the trapping data alone (Borchers and Efford, 2008), and by maximizing (2) that uses the trapping data and sightings only of marked animals.

The MLE of density from trapping data was high and also imprecise, as expected from the sparsity of recaptures (Table 1). Naive MLE including sighting data were much lower; their apparently high precision is an artifact of spatial overdispersion. MPLE estimates using simulation-based $\hat{c}$ were higher than naive MLE, and their confidence intervals were more credible (Table 1). Modeling the sightings as binary data rather than counts had little effect on the MPLE. The alternative strategy of modeling only $\boldsymbol{\omega}$, the detection histories of the $n = 80$ marked rats across the marking and sighting phases, does not suffer from spatial overdispersion (Section 3.1). However, discarding counts of unmarked rats and unidentified marked rats sacrifices potentially valuable information. Estimates of rat density from the reduced dataset were intermediate in precision and magnitude between trapping-only estimates and MPLE using all sightings (Table 1).

7. Simulation Experiments

Some simulations are presented to illustrate the performance of MPLE. Limited simulations are also presented to evaluate the effect of mis-specifying the spatial distribution of marked animals and to compare MPLE (ignoring covariation among counts of unmarked sightings) with Bayesian analysis of the full model. The population N is assumed fixed (binomial n)

Table 1

Estimates of rat population density λ (95% CI) from spatial capture–recapture and capture–mark–resight models. Simulation-based estimates of overdispersion $\hat{c}$ used in maximum pseudolikelihood estimates (MPLE) are shown for sightings of unmarked rats (T) and marked but unidentified rats (T'). RSE = relative standard error.

Data	Estimator	$\hat{\lambda}$ ha^{-1}	$\widehat{\text{RSE}}(\hat{\lambda})$	$\hat{c}(T)$	$\hat{c}(T')$
Trapping only	MLE	33.9 (22.3, 51.6)	0.217	–	–
Trapping + marked sightings	MLE	22.6 (16.2, 31.6)	0.172	–	–
All data (count)	naive MLE	17.7 (16.1, 19.6)	0.050	–	–
	MPLE	20.9 (17.3, 25.3)	0.097	22.8	19.0
All data (binary)	naive MLE	14.2 (12.3, 16.4)	0.074	–	–
	MPLE	20.3 (16.6, 24.8)	0.104	10.0	8.4

to allow comparison with published results (e.g., Royle et al., 2014).

7.1. *Validation of Models*

Two detector configurations were considered: a 6×6 square array of binary proximity detectors, and a 10×10 array of the same detectors. The scale parameter σ was set equal to the array spacing. A fixed population of $N = 200$ animals was distributed uniformly within a square extending 4σ beyond the detectors. The intercept parameter of the half-normal detection function was $h_0 = 0.2$. Two types of sampling were simulated: marking of a random sample of animals detected on a single occasion, followed by five resighting occasions, and pre-marking of exactly $n_0 = 50$ individuals distributed uniformly over the arena, also followed by five resighting occasions.

The relevant model from Section 3 or Section 4 was fitted to each of 500 replicate datasets. Sighting-only models were fitted to the pre-marked samples assuming n_0 was either known (allowing some detection histories to be all-zero) or unknown. Integrals were approximated by the sum over a 32×32 grid of pixels extending 4σ beyond the detectors. Estimators were evaluated with respect to relative bias (RB), relative standard error (RSE), relative root-mean-square error (rRMSE), and coverage of 95% confidence intervals (COV).

The average bias of the naive MLE estimates was small ($< 3\%$), but coverage of nominal 95% log-normal confidence intervals was poor (0.75–0.91) for the naive estimator, especially for models that included the marking phase (Table 2). Unmarked sightings were substantially overdispersed ($3.65 \leq \hat{c} \leq 4.29$). The coverage of 95% MPLE confidence intervals was close to the nominal level (0.93–0.97; Table 2).

7.2. *Effect of Mis-Specifying the Distribution of Marked Animals*

For sighting-only models, it is necessary to specify the distribution of marked animals $\pi(\mathbf{s})$. If the marked sample is obtained by passive sampling at fixed detectors then the distribution depends on the unknown values of the detection parameters (Figure 1). Simulations were conducted to determine the effect of mis-specifying $\pi(\mathbf{s})$ as uniform over various subsets of the area of integration. Simulation conditions were as for the 6×6 and 10×10 arrays of the preceding section; data from the marking occasion were either used in a full analysis (capture–mark–resight) or discarded (mark–resight). For mark–resight analyses, the distribution of marked animals was specified either as uniform over a square area A_0 extending a multiple of σ beyond the detector array (width w). 500 simulations were performed for each scenario.

Mark–resight estimates with an incorrectly specified distribution of marks showed large bias and poor confidence interval coverage (Web Table 4). The bias varied from positive to negative with increasing A_0. In these scenarios, bias was low for $A_0 \approx (w + 2\sigma)^2$, but the zero-bias boundary is likely to change with sampling intensity.

7.3. *Consequences of Ignoring Covariation of Unmarked Counts*

The spatial model of Chandler and Royle (2013) for sightings of a partially marked population was fitted to sighting data from 6×6 and 10×10 arrays allowing for a known number of marked individuals ($n_0 = 50$), generated as in the second group of simulations in Table 2, but using Poisson-distributed counts rather than binary data. The data augmentation parameter M was set to 500 individuals, allowing significant "headroom" over the fixed population ($N = 200$). Other simulation conditions followed their Section 4.1 (specifically, uninformative priors and 32,000 posterior samples, discarding the first 2000). Computation used a slightly modified version of the Chandler and Royle algorithm (Web Appendix F).

The Bayesian estimator including covariation of unmarked counts was slightly less biased than the MPLE for the particular sightings-only scenarios tested here (Table 3). More extensive simulations (Web Appendix A) support the

Table 2

Simulation results for maximum likelihood estimator of density from capture–mark–resight and mark–resight spatial data. The fitted model matched that used to generate the data except that covariation of the multivariate Poisson process for unmarked animals was either ignored ("Naive MLE") or considered only via weighting for overdispersion in the pseudolikelihood ("MPLE"). RB = relative bias, RSE = relative standard error, COV = coverage of 95% log-normal confidence intervals. 500 replicates. n number of animals marked, $\sum \boldsymbol{\omega}$ number of detections of marked individuals, including first, T number of sightings of unmarked animals.

				Naive MLE			MPLE		
Model and detector(s)	n	$\sum \boldsymbol{\omega}$	T	RB	RSE	COV	RB	RSE	COV
Capture–mark–resight									
6×6 array	36.7	187	86	−0.017	0.103	0.842	−0.006	0.132	0.954
10×10 array	55.9	335	137	−0.024	0.072	0.748	−0.020	0.100	0.972
Mark–resight, known n_0									
6×6 array	–	64	118	−0.001	0.150	0.912	0.017	0.176	0.942
10×10 array	–	102	231	−0.015	0.102	0.874	−0.019	0.123	0.944
Mark–resight, unknown n_0									
6×6 array	–	64	119	0.000	0.176	0.904	0.026	0.199	0.934
10×10 array	–	103	231	−0.027	0.109	0.896	−0.016	0.129	0.928

n, $\sum \boldsymbol{\omega}$, T are averages over replicates, SE 0.3–2.0. Average overdispersion $\hat{c}$ 3.6–4.3.

Table 3

Comparison of spatial population size estimators for simulated mark–resight data (true $N = 200$). Covariation of the multivariate Poisson process for unmarked animals was modeled directly ("Bayesian") or considered only as an adjustment for overdispersion in a pseudolikelihood ("MPLE," from Table 2). COV is the coverage of 95% log-normal confidence intervals for the MPLE, and 95% credible intervals for the Bayesian estimates. In the Bayesian case RB and rRMSE refer to the relative bias and relative root-mean-square error of the mode of the posterior distribution (200 replicates).

	MPLE			Bayesian		
Detectors	RB	rRMSE	COV	RB	rRMSE	COV
6 × 6 array	0.017	0.182	0.942	0.028	0.185	0.935
10 × 10 array	−0.019	0.124	0.944	0.005	0.121	0.940

conclusion of Chandler and Royle (2013) that allowing for the covariance structure significantly improves estimation when few animals are marked and $\sigma \approx 0.5s$, where s is the detector spacing. However, estimation by MPLE was at least 20 times faster (Web Table 3).

8. Discussion

The spatial capture–mark–resight (SCMR) models in this article extend current MLE methods for spatially explicit capture–recapture. The foremost issue in modeling spatial mark–resight data is the (usually unknown) spatial distribution of marked animals. This is resolved in SCMR by including a spatial submodel for the initial capture and marking; SMR models that rely instead on an assumed distribution for the marked animals can be justified only in special cases. SCMR and SMR methods that maximize a proposed pseudolikelihood with weighting for spatial overdispersion have been packaged in software alongside likelihood-based SECR methods (Efford, 2017). For the SMR puma dataset of Kelly et al. (2008), we show in Web Appendix E that the pseudolikelihood approach gives similar estimates to Bayesian methods (Sollmann et al., 2013b; Royle et al., 2014). Recent work by Whittington et al. (in press) has extended the Bayesian approach to include spatial capture–mark–resight models in our terminology, with promising results. We consider the methodologies to be complementary and mutually illuminating. Further work on SCMR and SMR models is needed to address other issues that arise in field studies such as population turnover and the inclusion of telemetry data.

8.1. *Rat Population Estimation Using Trapping and Motion-Activated Cameras*

Our rat data are likely to be typical of many field studies in which few recaptures are made during the marking phase and sightings are far more numerous. Under these conditions, the inclusion of sighting data substantially improves the precision of density estimates. However, we encountered problems in the rat sighting data that potentially introduced bias, and that may be common in field studies. Specifically, (i) the status of many sightings was uncertain, and it may not be correct to assume that doubtful sightings of marked and unmarked animals were discarded with equal probability, and (ii) subtle home-range shifts may occur between the marking and sighting phases. We do not believe these factors caused significant bias in our estimates of rat density, but we had no independent check. Whittington et al. (in press) analyzed comparable data from a study of grizzly bears (*Ursus arctos*). They found it difficult to fit models to count data by MCMC sampling, a problem they attributed to (non-spatial) overdispersion. They avoided this problem by casting the data as binary. There may well have been non-spatial overdispersion in the rat data (repeated sightings of an animal in close succession were unlikely to be independent), but it did not impede MPLE, and the estimates from binary and count analyses were very similar.

8.2. *Area Search*

The sighting models of Sections 3 and 4 may be applied almost unchanged to sightings gathered by searching a defined area, treating each searched polygon as a "detector." In Web Appendix D, we analyzed data from a study by J. Hill in which plots were searched for grassland sparrows. Area-search data may also be analyzed by discretizing the area as a number of small pixels and treating each pixel as a point detector. Another interesting possibility for the sightings of unmarked animals from area searches is to model them as a clustered spatial point process, substituting the Palm pseudolikelihood for L_T in equation (1) (Tanaka, Ogata, and Stoyan, 2008; Fewster, Stevenson, and Borchers, 2016).

8.3. *Capture–Mark–Resight and Mark–Resight Spatial Data*

The need to specify the spatial distribution of marked animals is a weakness of mark–resight models, and misspecification can be damaging (Web Table 4; Royle et al., 2014; Whittington et al., in press). Under some conditions the distribution of marked animals may be known or reasonably assumed. In the puma analysis of Web Appendix E, for example, the fraction of naturally pre-marked animals was assumed constant over space. Joint modeling of the marking and sighting phases also removes this problem, as the marking data and model implicitly determine the spatial distribution of marked animals, given the assumption that animals do not shift their home ranges.

Joint modeling of marking and sighting has further advantages. It deals naturally with occasion–occasion changes in the distribution of marked animals when marking and sighting occasions are interspersed, even if animals are trapped sequentially in different parts of a study area. Interspersion likely increases robustness to minor home-range shifts, although we note that, given population closure, the number of resightings is maximized by concentrating marking effort at the start of a study. A joint model fitted to pilot data may be used to optimize the study design by simulating scenarios for the allocation of effort between marking and sighting phases, and across space. This last point regarding study design is critical, as even numerous sightings of unmarked animals may sometimes contribute little to overall precision.

8.4. *Spatial Information in Sightings of Unmarked Animals*

We have based estimation on a likelihood that discards information in the spatial correlations among counts of sightings of unmarked animals $\{T_{jk}\}$. This is purely a matter of convenience. Pairwise composite likelihood methods (Varin, Reid, and Firth, 2011) may be developed in future to model the covariance structure of the counts.

We have shown that the cost of this model mis-specification may be largely eliminated by maximizing a pseudolikelihood in which the sighting component is weighted inversely by a simulation-based estimate of spatial overdispersion. However, we still expect to sacrifice some precision in the estimate of density, as the information discarded is what allowed Chandler and Royle (2013) to obtain crude estimates of density from datasets with no marked animals at all. The loss-of-precision handicap will be greater for SMR models than SCMR models as the former rely entirely on sightings. We therefore, address the magnitude of the handicap for SMR.

Simulation experiments showed that loss of precision in SMR models depends strongly on context. Our principal simulations found the MPLE to be marginally less precise than the corresponding point estimates from MCMC and data augmentation (Table 3). Chandler and Royle (2013) and Royle et al. (2014, Tables 19.3, 19.4) showed for particular scenarios involving small numbers of marked individuals that allowing for the covariance of the unmarked counts could substantially increase precision. Further work is needed to map the region in parameter- and design-space for which the spatial covariance of $\{T_{jk}\}$ contributes significant information for the estimation of density. We suspect that the covariance structure provides a useful signal only under quite strict conditions. For example, Chandler and Royle (2013) noted a rapid loss of precision as σ increased from 0.5 to 1.0 times detector spacing. The 15 × 15 detector array in their simulations was larger than those in common use, and the simulated population was sparse relative to σ, resulting in low overlap between home ranges. Intuitively, either condition might enhance the signal from spatial covariance of unmarked counts. Efford et al. (2016) suggested $k = \sigma\sqrt{\lambda}$ as an index of overlap assuming a random distribution of centres; for the Chandler and Royle simulations with $\sigma = 0.5$, we find $k \approx 0.22$, which is less than estimated from population studies of solitary carnivores, small mammals and forest birds (Efford et al., 2016; unpublish. results).

8.5. *Compatibility of Sightings and Data on Marked Animals*

Joint modeling of marking and sighting data relies on the constancy of shared parameters and home-range centres, and on the assumption that no births, deaths, immigration, or emigration occur between marking and sighting. The spatially overdispersed sightings of unmarked animals carry more weight in the naive model than is justified by their information content, which is overcome by down-weighting these data in the pseudolikelihood. The joint model may still represent a poor compromise between disparate data sets, and further work is needed to evaluate measures of goodness-of-fit (Royle et al., 2014). If counts of unmarked sightings are unreliable then it may be desirable to discard them and rely only on sightings of marked animals (e.g., "Trapping + marked sightings" in Table 1). A particular issue arises when home-range centres shift between the marking and sighting phases. In a model that treats centres as fixed, the implied location of the overall latent center is biased towards the center for whichever of the marking and sighting phases has the larger number of observations. A phase-specific model for σ then shows a spuriously large $\hat{\sigma}$ in the other phase.

8.6. *Comments on Heterogeneous Detection*

McClintock et al. (2009b) developed non-spatial mark–resight estimators that include a random effect for variation in detection probability to address concerns about bias driven by individual heterogeneity. Heterogeneity of the parameters h_0 and σ among individuals is also likely to bias estimates of density from capture–mark–resight and mark–resight spatial data. A continuous random effect might be introduced for these parameters, or each might be represented by a finite mixture (Pledger, 2000; Borchers and Efford, 2008; Efford, 2017). For SECR the critical heterogeneity is in the individual-level effective sampling area $a(\boldsymbol{\theta})$ (Section 5.3) which for a given sampling design is a function of both h_0 and σ (Efford and Mowat, 2014). There is not a direct analogue of $a(\boldsymbol{\theta})$ for mark–resight models owing to their more complex structure and the lack of a Horvitz–Thompson-like estimator that includes counts of unmarked animals. The possible interaction between heterogeneity and failure to identify marked individuals (p_I) requires investigation in spatial models (cf, McClintock et al., 2014).

9. Supplementary Materials

Web Appendices and Tables referenced in Sections 3, 6, 7, and 8 are available with this article at the *Biometrics* website on Wiley Online Library. The R code used to perform the simulations in Section 7 is described in Web Appendix F.

ACKNOWLEDGEMENTS

David Fletcher contributed valuable insights on overdispersion. The rat study was conducted by Claire Kilner, Josh Kemp, Graeme Elliott, and others; we thank them and Jason Hill, Duane Diefenbach, Marcella Kelly, and Lindsey Rich for generously providing access to data. Thanks, also to Rahel Sollmann and anonymous reviewers for their many helpful comments on a earlier draft.

REFERENCES

Borchers, D. L. and Efford, M. G. (2008). Spatially explicit maximum likelihood methods for capture–recapture studies. *Biometrics* **64**, 377–385.

Borchers, D. L. and Fewster, R. M. (2016). Spatial capture–recapture models. *Statistical Science* **31**, 219–232.

Chandler, R. B. and Royle, J. A. (2013). Spatially explicit models for inference about density in unmarked or partially marked populations. *Annals of Applied Statistics* **7**, 936–954.

Efford, M. G. (2011). Estimation of population density by spatially explicit capture–recapture analysis of data from area searches. *Ecology* **92**, 2202–2207.

Efford, M. G. (2017). secr: Spatially explicit capture-recapture models. R package version 3.0.1. `http://CRAN.R-project.org/package=secr` [accessed 23 May 2017].

Efford, M. G., Borchers, D. L., and Byrom, A. E. (2009). Density estimation by spatially explicit capture–recapture: Likelihood-based methods. In *Modeling Demographic Processes in Marked Populations*, D. L. Thomson, E. G. Cooch, and M. J. Conroy (eds), 255–269. New York: Springer.

Efford, M. G., Dawson D. K., and Borchers, D. L. (2009). Population density estimated from locations of individuals on a passive detector array. *Ecology* **90**, 2676–2682.

Efford, M. G., Dawson, D. K., Jhala, Y. V., and Qureshi, Q. (2016). Density-dependent home range size revealed by spatially explicit capture–recapture. *Ecography* **39**, 676–688.

Efford, M. G. and Mowat, G. (2014). Compensatory heterogeneity in spatially explicit capture–recapture data. *Ecology* **95**, 1341–1348.

Fewster, R. M., Stevenson, B. C., and Borchers, D. L. (2016). Trace-contrast models for capture–recapture without capture histories. *Statistical Science* **31**, 245–258.

Kelly, M. J., Noss, A. J., Di Bitetti, M. S., Maffei, L., Arispe, R. L., Paviolo, A., et al. (2008). Estimating puma densities from camera trapping across three study sites: Bolivia, Argentina, and Belize. *Journal of Mammalogy* **89**, 408–418.

Matechou, E., Morgan, B. J. T., Pledger, S., Collazo, J. A., and Lyons, J. E. (2013). Integrated analysis of capture–recapture–resighting data and counts of unmarked birds at stop-over sites. *Journal of Agricultural, Biological, and Environmental Statistics* **18**, 120–135.

McClintock, B. T., Hill, J. M., Fritz, L., Chumbley, K., Laxa, K., and Diefenbach, D. R. (2014). Mark–resight abundance estimation under incomplete identification of marked individuals. *Methods in Ecology and Evolution* **5**, 1294–1304.

McClintock, B. T. and White, G. C. (2009). A less field intensive robust design for estimating demographic parameters with mark–resight data. *Ecology* **90**, 313–320.

McClintock, B. T. and White, G. C. (2012). From NOREMARK to MARK: Software for estimating demographic parameters using mark–resight methodology. *Journal of Ornithology* **152**, S641–S650.

McClintock, B. T., White, G. C., Antolin, M. F., and Tripp, D. W. (2009a). Estimating abundance using mark–resight when sampling is with replacement or the number of marked individuals is unknown. *Biometrics* **65**, 237–246.

McClintock, B. T., White, G. C., Burnham, K. P., and Pryde, M. A. (2009b). A generalized mixed effects model of abundance for mark-resight data when sampling is without replacement.In *Modeling Demographic Processes in Marked Populations*, D. L. Thomson, E. G. Cooch, and M. J. Conroy (eds), 271–289. New York: Springer.

Pledger, S. (2000). Unified maximum likelihood estimates for closed capture–recapture models using mixtures. *Biometrics* **56**, 434–442.

R Core Team (2016). *R: A language and environment for statistical computing.* R Foundation for Statistical Computing, Vienna, Austria. `http://www.R-project.org/`

Rich, L. N., Kelly, M. J., Sollmann, R., Noss, A. J., Maffei, L., Arispe, R. L., et al. (2014). Comparing capture–recapture, mark–resight, and spatial mark–resight models for estimating puma densities via camera traps. *Journal of Mammalogy* **95**, 382–391.

Royle, J. A., Chandler, R. B., Sollmann, R., and Gardner, B. (2014). *Spatial Capture–Recapture.* Waltham, Massachusetts: Academic Press.

Royle, J. A. and Young, K. V. (2008). A hierarchical model for spatial capture–recapture data. *Ecology* **89**, 2281–2289.

Sollmann, R., Gardner, B., Chandler, R. B., Shindle, D., Onorato, D. P., Royle, J. A., et al. (2013a). Using multiple data sources provides density estimates for endangered Florida panther. *Journal of Applied Ecology* **50**, 961–968.

Sollmann, R., Gardner, B., Parsons, A. W., Stocking, J. J., McClintock, B. T., Simons, T. R., et al. (2013b). A spatial mark-resight model augmented with telemetry data. *Ecology* **94**, 553–559.

Tanaka, U., Ogata, Y. and Stoyan, D. (2008). Parameter estimation and model selection for Neyman–Scott point processes. *Biometrical Journal* **50**, 43–57.

Varin, C., Reid, N., and Firth, D. (2011). An overview of composite likelihood methods. *Statistica Sinica* **21**, 5–42.

Whittington, J., Hebblewhite, M., and Chandler, R. B. (2017). Generalized spatial mark–resight models with an application to grizzly bears. *Journal of Applied Ecology* In press.

Received January 2016. *Revised July* 2017. *Accepted July* 2017.